Sigma J Eng & Nat Sci 37 (2), 2019, 393-413

Sigma Journal of Engineering and Natural Sciences
Sigma Mühendislik ve Fen Bilimleri Dergisi

Research Article

INVESTIGATION OF MICROPOLAR FLUID FLOW AND HEAT TRANSFER IN A TWO-DIMENSIONAL PERMEABLE CHANNEL BY ANALYTICAL AND NUMERICAL METHODS

Mosayeb GHOLINIA*[1], Saber GHOLINIA[2], Hossein JAVADI[3], Davood Domiri GANJI[4]

[1]*Babol Noshirvani University of Technology, Faculty of Mechanical Engineering, Babol-IRAN;*
ORCID: 0000-0001-8291-8824
[2]*Babol Noshirvani University of Technology, Faculty of Mechanical Engineering, Babol-IRAN;*
ORCID: 0000-0003-4597-2279
[3]*Mazandaran University of Science and Technology, Faculty of Mechanical Engineering, Babol-IRAN;*
ORCID: 0000-0002-2059-7145
[4]*Babol Noshirvani University of Technology, Faculty of Mechanical Engineering, Babol-IRAN;*
ORCID: 0000-0002-4293-5993

Received: 09.07.2018 Revised: 07.03.2019 Accepted: 09.04.2019

ABSTRACT

In this paper, we have used the Variational Iteration Method (VIM) to study micropolar fluid flow and heat transfer in a two-dimensional permeable channel. To check the precision of the obtained results, they have been compared with the results of Runge-Kutta Fourth-Order Method, Akbari-Ganji's Method (AGM), Collocation Method (CM), and Flex-PDE software. The influences of various parameters including microrotation/angular velocity, Peclet number (Pe), and Reynolds number (Re) on the flow, concentration, and heat transfer distribution are studied. Based on the results, Nusselt number (Nu) has a direct relation with Reynolds number and Sherwood number (Sh), while it has a reverse relation with Peclet number. In addition, by increasing Peclet number, concentration and temperature profiles increase as well. It is concluded that both VIM and AGM are powerful methods to solve nonlinear differential equations.
Keywords: Micropolar fluid, permeable channel, Variational Iteration Method (VIM), Akbari-Ganji's Method (AGM), heat transfer.

1. INTRODUCTION

In the field of fluid mechanics, researchers are studying the particles behavior at various physical conditions. In most issues, particularly in engineering, mathematical models have been widely used to describe scientific phenomena for a variety of fluids like non-Newtonian and Newtonian fluids. There are many non-Newtonian fluids such as micropolar fluids and nanofluids. Micropolar fluids have special structures in which the velocity field and the macroscopic rotation of each particle are coupled. A hydrodynamical framework is appropriate for granular systems which consist of particles on a macroscopic scale. Micropolar fluids include

* Corresponding Author: e-mail: m.gholinia1371@gmail.com, tel: +98 (919) 9198246

rigid and randomly oriented particles that spin and have microrotation velocity and are suspended in a viscous medium. The theory of a micropolar fluid derives from a requirement to model the flow of fluids that have rotating micro-constituents. Eringen [1] was the first pioneer of formulating the theory of micropolar fluids. His idea introduced modern material parameters, microrotation velocity, an additional independent vector field and new constitutive equations for Newtonian fluid flow which must be solved simultaneously via the usual equations. He [2] extended the theory of thermos micropolar fluids and derived the constitutive laws for fluids having microstructure. The popularity of micropolar fluids might be because of the fact that they are a simple and impressive generalization of Navier-Stokes equation. Micropolar fluid problems can be studied in different applications like solidification of human and animal blood (Ariman et al. [3]), liquid crystals (Lockwood et al. [4]) cooling of a metallic sheet in a bath, flow of low concentration suspensions, production of paper and glass, lubrication components, colloidal fluids etc. Moreover, micropolar fluids are used to model the fluid flow at micro scales in systems including micropumps, accelerometers, microsensors, and microresonators, which have various applications in the fields of aerospace, biomechanics, petrochemicals, and medicine. The widespread uses of micropolar fluids have been presented in the books of Eringen [5] and Lukaszewicz [6]. Most scholars have studied different issues in micropolar fluids, such as Gorla [7], Rees and Bassom [8] who studied the flow of a micropolar fluid over a flat sheet. In addition, Kelson and Desseaux [9] investigated the micropolar fluids flow on stretching surfaces. Bhargava et al. [10] presented finite element solutions for a mixed convective micropolar flow in a porous plate. Stagnation point of a micropolar fluid towards a stretching plate was studied by Nazar et al. [11]. Joneidi et al. [12] studied the behavior of micropolar fluid flow in a porous channel with the high mass transfer. Heat transfer issues in micropolar fluids flow have been analyzed by Perdikis and Raptis [13,14] who also investigated the impacts of heat radiation. Balaram and Sastry [15] examined the fully extended free convection flow of a micropolar fluid. Mohanty et al. [16] investigated mass and heat transfer effects of a micropolar fluid over stretching plate numerically. The impact of Hall effect and thermal radiation on mass and heat transfer of a Magnetohydrodynamic (MHD) flow of a micropolar fluid in a porous medium was studied by Oahimire and Olajuwa [17]. Based on iterative power series solutions, Al Sakkaf et al. [18] studied the unsteady viscous flow over a contracting cylinder. It found to be that the new method is powerful for systems that are defined by nonintegrable nonlinear differential equations. An investigation on the free convective micropolar fluid over a shrinking sheet was carried out by Mishra et al. [19] considering a heat source/sink. It was concluded that using heat source resulted in a decrease in the boundary layer and a considerable influence on the velocity profile (See also [20, 21]).

Moreover, in recent years some scholars have examined micropolar fluid, nanofluid and their effects [22-29]. Because of the nonlinear nature of micropolar fluids, solving problems related to these fluids has been a controversial challenge for engineers, physicists, and mathematicians. Many methods have been presented to study the nonlinear problems including Optimal Homotopy Analysis Method (OHAM) [30], Exp-Function Method (EFM) [31,32], Since-Cosine Function Method (SCFM) [33,34], Homotopy Analysis Method (HAM) [35,36], F-Expansion Method (FEM) [37,38], Tanh-Coth Method (TCM) [39,40], Control Volume based Finite Element Method (CVFEM) [41,42], Akbari-Ganji's Method (AGM) [43-45], and He's Frequency–amplitude Formulation Method (HFFM) [46], etc. In recent years, Variational Iteration Method (VIM), which is actually the modified form of Lagrange multipliers, has been widely used to solve nonlinear problems. The basic idea of the method is based on Inokuti-Sekine-Mura method [47] developed by He [48]. This method was considered interesting due to its simplicity and high accuracy and efficiency in finding analytical solutions for linear and nonlinear problems. After that, some modifications were applied in order to overcome the disadvantages resulting from solution steps by several researchers. For example, Abassy et al. [49,50] proposed modification by using Padé approximant and Laplace tran sform. In addition, Soltani and Shirzadi [51] applied new modifying procedures on VIM which provided great freedom in choosing linear operators for various nonlinear equations. Such technology was also suggested by He [52-54] for nonlinear oscillators.

Therefore, VIM is a strong manner for solving nonlinear differential equations like a presented equation in this study. In this paper, we have applied VIM to find the approximate solutions of nonlinear differential equations governing the micropolar fluid flow and heat transfer in a permeable channel. As well as, the concentration, velocity, and temperature profiles are shown and the impact of Peclet number, microrotation/angular velocity and Reynolds numbers on the flow, concentration, and heat transfer distribution are studied. To check the precision of the obtained results of VIM, they have been compared with the results of the numerical method (Runge-Kutta fourth-order method), Akbari-Ganji's Method (AGM), Collocation Method (CM), and Flex-PDE software. Furthermore, the timings of the aforementioned methods are presented in this paper for better use of the methods for solving nonlinear problems.

2. MATHEMATICAL FORMULATION OF THE PROBLEM

We have considered the steady laminar flow of a micropolar fluid along with a two-dimensional channel with porous walls in which fluid is uniformly removed or injected with speed V_0. The upper wall has a temperature T_2 and solute concentration C_2 while the lower wall has a temperature T_1 and solute concentration C_1 as shown in Fig. 1.

Using Cartesian coordinates, the channel walls are parallel to the x-axis and located at y=±h where 2h is the channel width. The relevant equations governing the flow are as follows [55]:

$$\frac{\partial u}{\partial x}+\frac{\partial v}{\partial y}=0, \tag{1}$$

$$\rho(u\frac{\partial u}{\partial x}+v\frac{\partial u}{\partial y})=-\frac{\partial p}{\partial x}+(\mu+k)(\frac{\partial^2 u}{\partial x^2}+\frac{\partial^2 u}{\partial y^2})+k\frac{\partial N}{\partial y}, \tag{2}$$

$$\rho(u\frac{\partial v}{\partial x}+v\frac{\partial v}{\partial y})=-\frac{\partial p}{\partial y}+(\mu+k)(\frac{\partial^2 v}{\partial x^2}+\frac{\partial^2 v}{\partial y^2})-k\frac{\partial N}{\partial x}, \tag{3}$$

$$\rho(u\frac{\partial N}{\partial x}+v\frac{\partial N}{\partial y})=-\frac{k}{j}(2N+\frac{\partial u}{\partial y}-\frac{\partial v}{\partial x})+(\frac{\mu_s}{j})(\frac{\partial^2 N}{\partial x^2}+\frac{\partial^2 N}{\partial y^2}), \tag{4}$$

$$\rho(u\frac{\partial T}{\partial x}+v\frac{\partial T}{\partial y})=\frac{k_1}{c_p}\frac{\partial^2 T}{\partial y^2}, \tag{5}$$

$$\rho(u\frac{\partial C}{\partial x}+v\frac{\partial C}{\partial y})=D^*\frac{\partial^2 C}{\partial y^2}. \tag{6}$$

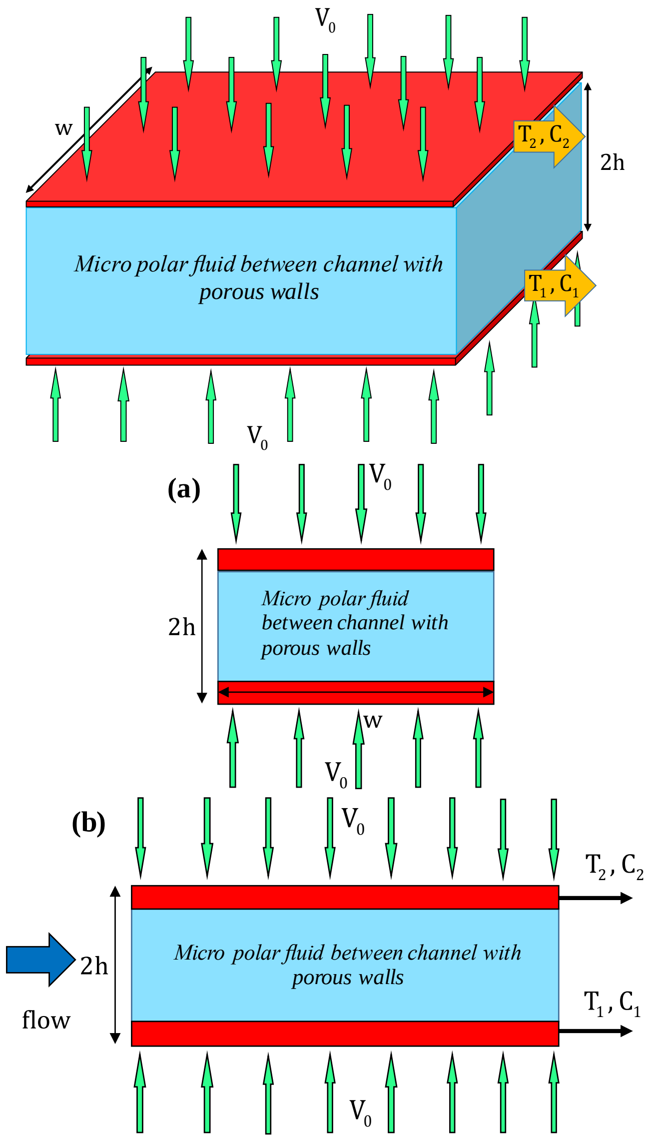

Figure 1. Schematic representation of the considered problem. **(a)** y-z view and **(b)** x-y view.

Where v and u are the velocity components along the y- and x-axis, respectively. μ is the dynamic viscosity, ρ is the fluid density, P is the fluid pressure, N is the angular or microrotation velocity, C is the species concentration, c_p and T are the specific heat at a constant pressure and temperature of the fluid, respectively. j is the microinertia density, k_1 and D* are the thermal conductivity and molecular diffusivity, respectively. Also, $vs = (\mu + k/2)j$ is the microrotation viscosity and k is a material parameter. The appropriate boundary conditions are as follows:

$$
\begin{aligned}
y &= -h \quad : \quad v = u = 0, N = -s\frac{\partial u}{\partial y} \\
y &= +h \quad : \quad v = 0, u = \frac{v_0 x}{h}, N = \frac{v_0 x}{h^2}
\end{aligned} \tag{7}
$$

Where *s* represents a degree in which the microelements are free to rotate near the channel walls. The case $s = 1$ represents the turbulent flow. Other interesting cases that have been considered in the present study include $s = 0.5$ which represents weak concentrations as well as vanishing condition of the anti-symmetric part of the stress tensor, and $s = 0$ which represents concentrated particle flows in which microelements are close to the wall and unable to rotate. We have introduced the following dimensionless variables [56]:

$$
\begin{aligned}
&\eta = \frac{y}{h}, \psi = -v_0 x f(\eta), N = \frac{v_0 x}{h^2} g(\eta), \\
&\theta(\eta) = \frac{T - T_2}{T_1 - T_2}, \phi(\eta) = \frac{C - C_2}{C_1 - C_2}.
\end{aligned} \tag{8}
$$

Where $C_2 = C_1 - Bx$, $T_2 = T_1 - Ax$ with *B* and *A* as constants. The stream function is defined in a usual way:

$$
u = \frac{\partial \psi}{\partial y}, v = -\frac{\partial \psi}{\partial x} \tag{9}
$$

Eqs. (1)-(8) are reduced to a coupled system of nonlinear differential equations:

$$
(1 + N_1) f^{IV} - N_1 g - \mathrm{Re}(f f''' - f' f'') = 0, \tag{10}
$$

$$
N_2 g'' + N_1 (f'' - 2g) - N_3 \mathrm{Re}(f g' - f' g) = 0, \tag{11}
$$

$$
\theta'' + Pe_h f' \theta - Pe_h f \theta' = 0, \tag{12}
$$

$$
\phi'' + Pe_m f' \phi - Pe_m f \phi' = 0, \tag{13}
$$

Subject to the boundary conditions:

$$
\begin{aligned}
\eta &= -1 \quad : \quad f = f' = g = 0, \ \theta = \phi = 1, \\
\eta &= +1 \quad : \quad f = \theta = \phi = 0, \ g = 1, \ f' = -1,
\end{aligned} \tag{14}
$$

The parameters of primary interest are Grashof number (*Gr*), and Reynolds number (*Re*), where for injection $\mathrm{Re} < 0$ and for suction $\mathrm{Re} > 0$. Peclet numbers for the diffusion of mass Pe_m and heat Pe_h are given, respectively:

$$N_1 = \frac{k}{\mu}, \qquad N_2 = \frac{v_s}{\mu h^2}, \qquad N_3 = \frac{j}{h^2}, \qquad \mathrm{Re} = \frac{v_0}{\upsilon} h,$$
$$\mathrm{Pr} = \frac{\upsilon \rho C_p}{k_1}, \qquad Sc = \frac{\upsilon}{D^*}, \qquad Gr = \frac{g \beta_T A h^4}{\upsilon^2}, \tag{15}$$
$$Pe_h = \mathrm{Pr}.\mathrm{Re}, \qquad Pe_m = Sc.\mathrm{Re},$$

where *Pr* is Prandtl number, *Sc* is the generalized Schmidt number, N_2 is the spin-gradient viscosity parameter and N_1 is the coupling parameter. In technological processes, the parameters of primary interest are the local Nusselt and Sherwood numbers. These are defined as follows:

$$Nu_x = \frac{q''_{y=-h} x}{(T_1 - T_2) k_1} = -\theta'(-1), \tag{16}$$

$$Sh_x = \frac{m''_{y=-h} x}{(C_1 - C_2) D^*} = -\phi'(-1). \tag{17}$$

Where m'' and q'' are local mass flux and heat flux, respectively.

3. APPLICATION OF VARIATIONAL ITERATION METHOD (VIM)

The Variational Iteration Method (VIM) gives the possibility to solve many types of nonlinear equations. To clarify its primary idea, we consider following differential equation:

$$L(U) + N(U) = g(x,t), \tag{18}$$

Where *N* is a nonlinear operator, *L* is a linear operator and *g(t)* is a given continuous function. According to this method, we can have a correction function as follows:

$$U_{n+1}(x,t) = U_n(x,t) + \int_0^t \lambda(L(U_n)(\xi) + N(\tilde{U}_n)(\xi) - g(\xi))d\xi, \qquad n \geq 0 \tag{19}$$

Where λ is a Lagrange multiplier which can be identified optimally via variational theory [57–59], U_n is the nth approximate solution, and $\tilde{U}_n$ denotes a restricted variation, i.e., $\delta \tilde{U}_n = 0$.

VIM is applied to solve the nonlinear differential equation (Eqs. (10)- (13)) with the selected boundary condition (Eq. (14)). In order to solve these equations using VIM, we have considered a correction function as follows:

$$f_{n+1}(x) = f_n(x) + \int_0^x \lambda_1(s)[(1+N_1) f_n^{IV}(s) - N_1 \tilde{g}_n(s) - \mathrm{Re}(\tilde{f}_n(s)\tilde{f}_n'''(s) - \tilde{f}_n'(s)\tilde{f}_n''(s))]ds,$$

$$g_{n+1}(x) = g_n(x) + \int_0^x \lambda_2(s)[N_2 g_n''(s) + N_1(\tilde{f}_n''(s) - 2\tilde{g}_n(s)) - N_3 \mathrm{Re}(\tilde{f}_n(s)\tilde{g}_n'(s) - \tilde{f}_n'(s)$$

$$\tilde{g}_n(s))]ds, \tag{20}$$

$$\theta_{n+1}(x) = \theta_n(x) + \int_0^x \lambda_3(s)\left[\theta_n''(s) + Pe_h \tilde{f}_n'(s)\tilde{\theta}_n(s) - Pe_h \tilde{f}_n(s)\tilde{\theta}_n'(s)\right]ds,$$

$$\phi_{n+1}(x) = \phi_n(x) + \int_0^x \lambda_4(s)\left[\phi''(s) + Pe_m \tilde{f}_n'(s)\tilde{\phi}_n(s) - Pe_m \tilde{f}_n(s)\tilde{\phi}_n'(s)\right]ds.$$

where λ(*s*) is Lagrange multipliers, which can be identified optimally via the variational theory. The stationary conditions can be obtained as follows:

$$\begin{aligned}
&1-\lambda_1'''(S)\big|_{s=x}=0, \quad \lambda_1''(S)\big|_{s=x}=0, \quad \lambda_1'(S)\big|_{s=x}=0, \quad \lambda_1(S)\big|_{s=x}=0,\\
&1-\lambda_2''(S)\big|_{s=x}=0, \quad \lambda_2(S)\big|_{s=x}=0,\\
&1-\lambda_3''(S)\big|_{s=x}=0, \quad \lambda_3(S)\big|_{s=x}=0,\\
&1-\lambda_4''(S)\big|_{s=x}=0, \quad \lambda_4(S)\big|_{s=x}=0.
\end{aligned} \tag{21}$$

The Lagrange multipliers can be identified as $\lambda_1(s)=(x-s)^3/6$, $\lambda_2(s)=\lambda_3(s)=\lambda_4(s)=(s-x)$ and the following variational iteration formula can be obtained:

$$f_{n+1}(x) = f_n(x) - \int_0^x (x-s)^3/6\,[(1+N_1) f_n^{IV}(s) - N_1\tilde{g}_n(s) - \mathrm{Re}(\tilde{f}_n(s)\tilde{f}_n'''(s)$$

$$-\tilde{f}_n'(s)\tilde{f}_n''(s))]ds,$$

$$g_{n+1}(x) = g_n(x) + \int_0^x (s-x)\,[N_2 g_n''(s) + N_1(\tilde{f}_n''(s) - 2\tilde{g}_n(s)) - N_3 \mathrm{Re}(\tilde{f}_n(s)\tilde{g}_n'(s)$$

$$-\tilde{f}_n'(s)\tilde{g}_n(s))]ds, \tag{22}$$

$$\theta_{n+1}(x) = \theta_n(x) + \int_0^x (s-x)[\theta_n''(s) + Pe_h \tilde{f}_n'(s)\tilde{\theta}_n(s) - Pe_h \tilde{f}_n(s)\tilde{\theta}_n'(s)]ds,$$

$$\phi_{n+1}(x) = \phi_n(x) + \int_0^x (s-x)[\phi''(s) + Pe_m \tilde{f}_n'(s)\tilde{\phi}_n(s) - Pe_m \tilde{f}_n(s)\tilde{\phi}_n'(s)]ds.$$

Now, we begin with arbitrary initial approximations:

$$f_0(x) = a_0 + a_1 x + a_2 x^2 + a_3 x^3,$$
$$g_0(x) = b_0 + b_1 x,$$
$$\theta_0(x) = c_0 + c_1 x, \tag{23}$$
$$\phi_0(x) = d_0 + d_1 x.$$

Where a_i, b_i, c_i, and d_i are constant in *x-axis* to be determined by using the boundary conditions. By using Eq. (31), we can obtain the following successive approximations:

$$f_1(x) = -0.0084x^4 a_1 a_2 - 0.0033x^6 a_2 a_3 + 0.025x^4 a_0 a_3 + 0.00084x^5 b_1 - 0.0033x^5 a_2{}^2$$
$$+0.00416x^4 b_0 + a_3 x^3 + a_1 x - 0.001428 a_3{}^2 x^7 + x^2 a_2 + a_0,$$
$$\text{g}_1(x) = b_1 x + b_0 - 0.001 a_3 b_1 x^5 - 0.00083x^4 a_2 b_1 - 0.00249x^4 a_3 b_0 - 0.1 a_3 x^3 + 0.034x^3 b_1$$
$$-0.0034x^3 a_2 b_0 - 0.1x^2 a_2 + 0.1x^2 b_0 + 0.005x^2 a_0 b_1 - 0.005x^2 a_1 b_0,$$
$$\theta_1(x) = c_1 x + c0 - 0.01 a_3 c_1 x^5 - 0.0083x^4 a_2 c_1 - 0.025x^4 a_3 c_0 - 0.0334x^3 a_2 c_0 - 0.05x^2 a_1 c_0$$
$$+0.05x^2 c_1 a_0, \tag{24}$$
$$\phi_1(x) = d_1 x + d0 - 0.01 a_3 d_1 x^5 - 0.0083x^4 a_2 d_1 - 0.025x^4 a_3 d_0 - 0.0334x^3 a_2 d_0 - 0.05x^2 a_1 d_0$$
$$+0.05x^2 d_1 a_0.$$

In the same manner, the rest of the components of the iteration formula can be obtained. Furthermore, we have solved this system for different values of $N_1, N_2, N_3, \text{Re}, Pe_h$, and Pe_m determined $a_0 ... a_3, b_0, b_1, c_0, c_1, d_0, d_1$ in each case. For example, when $N_1 = N_2 = N_3 = \text{Re} = Pe_h = Pe_m = 0.1$, we have:

$a_0 = 1/4,\ a_1 = 1/4,\ a_2 = -1/4,\ a_3 = -1/4, b_0 = 1/2,\ b_1 = 1/2,\ c_0 = 1/2,\ c_1 = -1/2,$
$d_0 = 1/2,\ d_1 = -1/2.$

4. SOLUTION BY FLEX-PDE SOFTWARE

Flex-PDE software is a modeling software based on the finite element method for coding. This software has the capability to analyze the wide range of engineering problems like chemical reaction kinetic, tension and modeling of real mathematical and engineering issues.

4.1. Precision control in Flex-PDE software

The advantage of this software is its precision control. Flex-PDE checks the compatibility of partial differential equations (PDEs) with the grid cells which results in estimating the relative error in the response variables and comparing it with the allowable limits of precision. If each one of the grid cells exceeds the allowable limit of error, that cell can be split and the solution process will be re-applied. Allowable limit of error is called ERRLIM in this software and its default value is 0.002. This means that Flex-PDE corrects the grid when the estimation error in each variable (in the range of changes of that variable) is less than 0.2 percent per cell. This shows that this software has excellent compatibility with numerical solutions. This software has rarely been used in the field of fluid mechanics and heat transfer so far. On the other hand, as this is open-source software, there is easy access to the dominant equations and it is possible to apply the desired changes to the equations or the material properties. In fact, the main capacity of this simple software is solving the complex nonlinear equations, which happens abundantly in the field of fluid mechanics and heat transfer. In this study, we have compared the outcomes of Flex-PDE software with outcomes of VIM, CM, and AGM by writing Flex-PDE codes for Eqs. (10)-(13).

5. RESULTS AND DISCUSSION

The comparison of the results of VIM with AGM, CM, Flex-PDE software, and numerical method (Runge-Kutta fourth-order method) has been carried out. Also, this investigation indicates that VIM and AGM are strong manners to solve nonlinear differential equations.

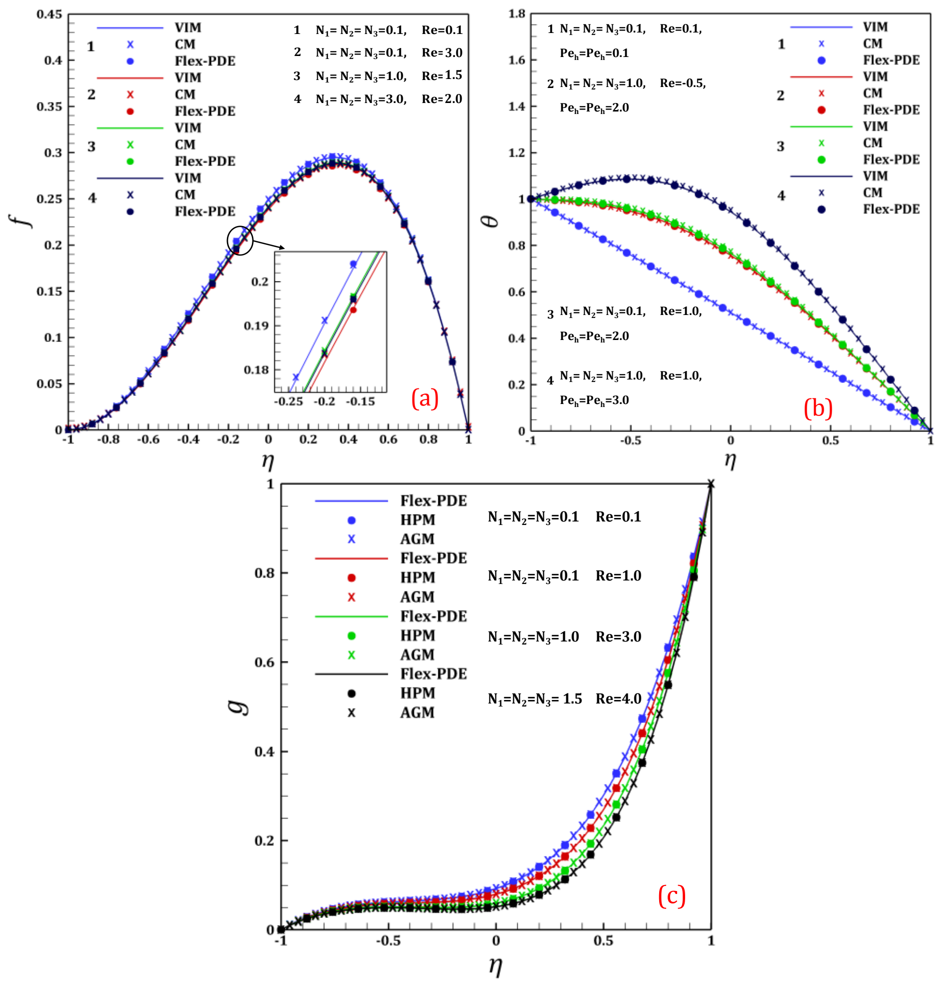

Figure 2. Comparison between the results of VIM, AGM, CM, and Flex-PDE software for (a) stream function (f), (b) temperature (θ), and (c) microrotation velocity (g).

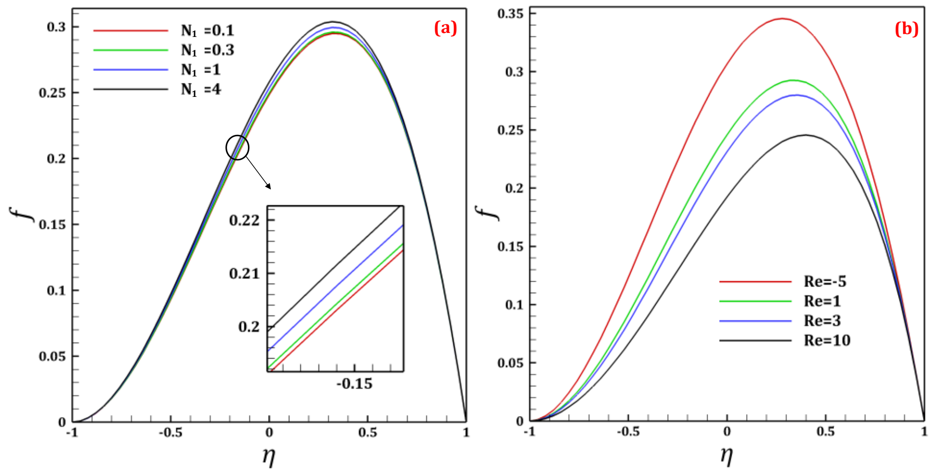

Figure 3. Impact of (a) N_1 and (b) Re on stream function (*f*).

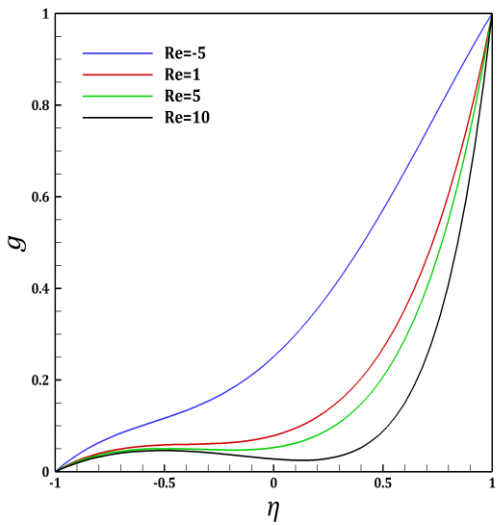

Figure 4. Impact of Re on microrotation velocity (*g*).

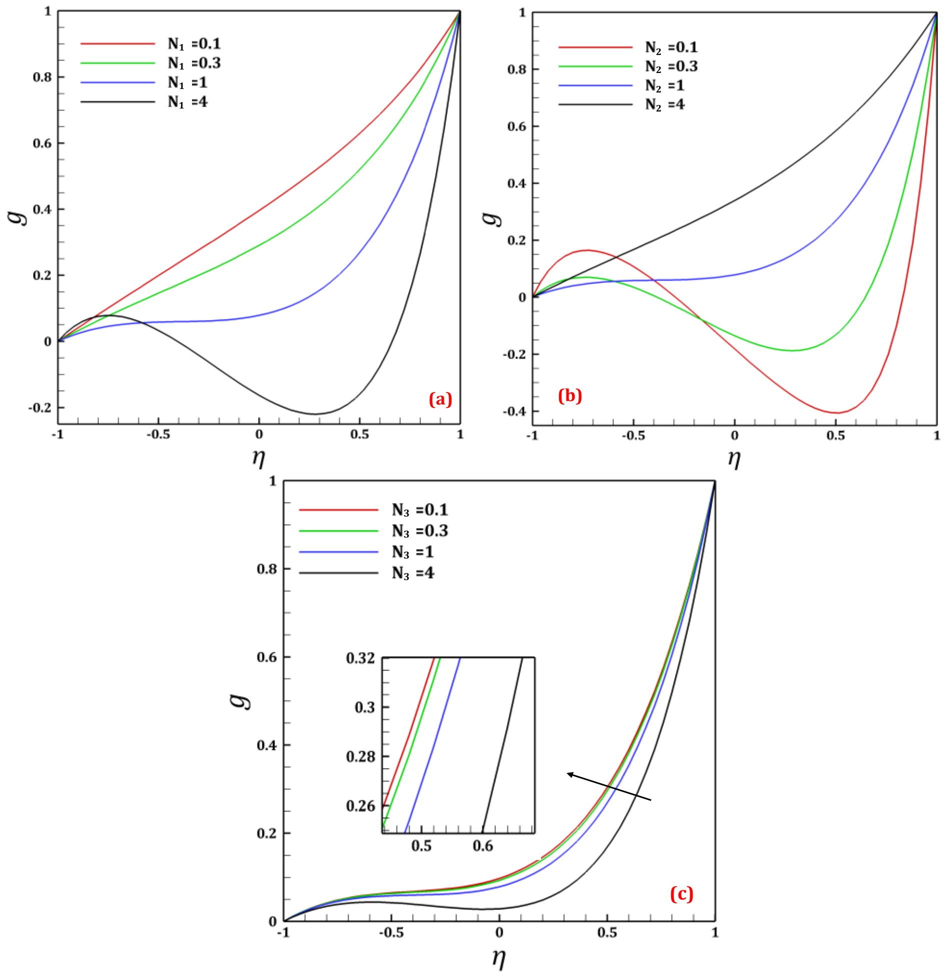

Figure 5. Impact of (a) N_1, (b) N_2, and (c) N_3 on microrotation velocity (g).

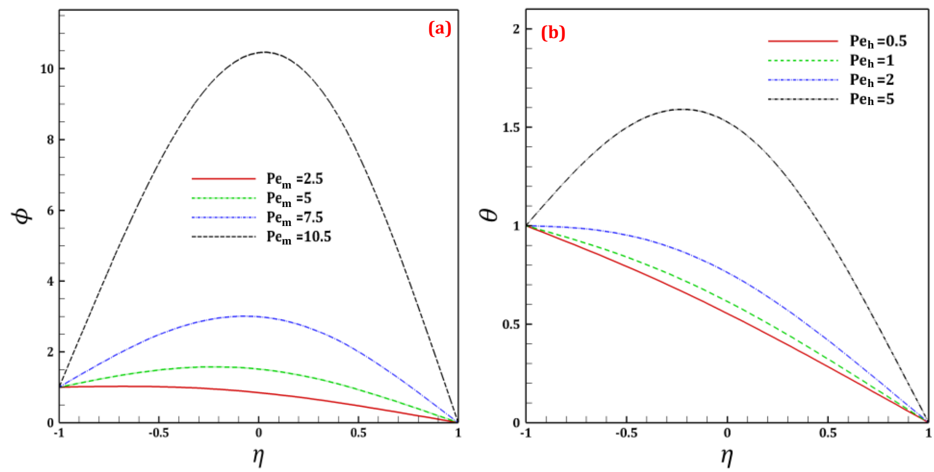

Figure 6. Impact of Peclet number on (a) concentration and (b) temperature distribution.

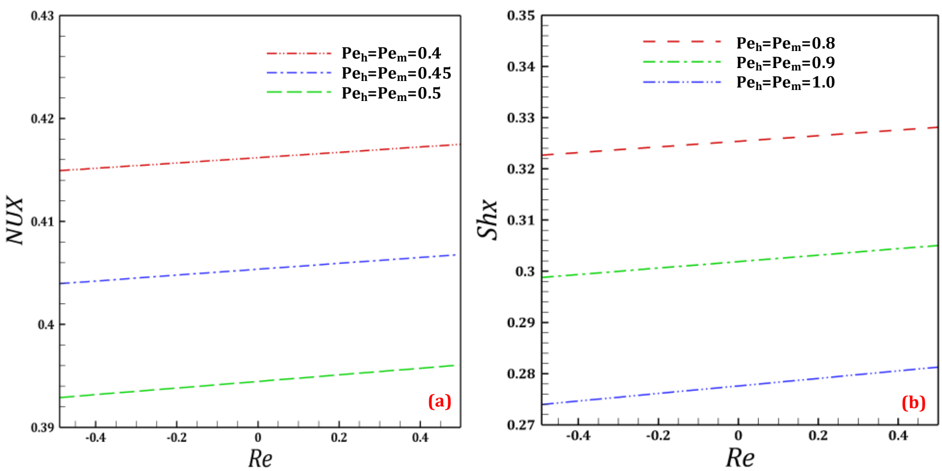

Figure 7. Impact of Peclet number and Reynolds number on (a) Nusselt number and (b) Sherwood number.

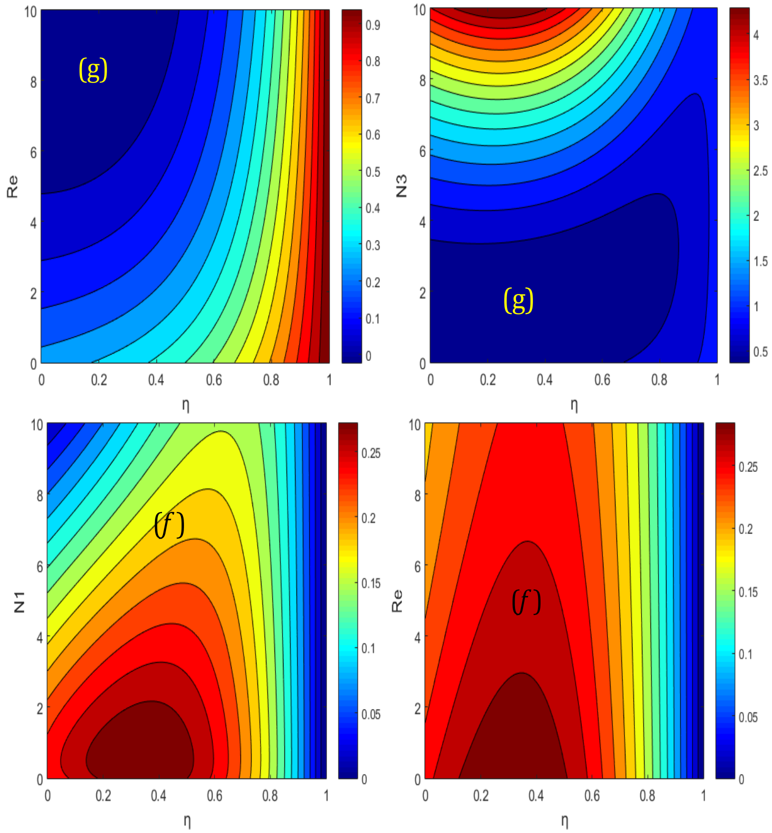

Figure 8. Contours of f (Right) and g (Left) when $N_1 = N_2 = N_3 = Pe_h = Pe_m = 1$.

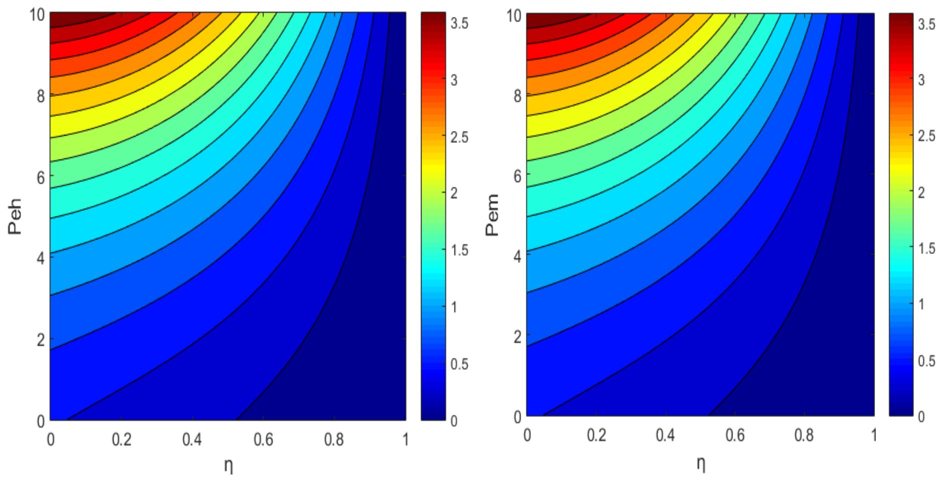

Figure 9. Contours of θ (Left) and ϕ (Right) when $N_1 = N_2 = N_3 = \mathrm{Re} = 1$.

Table 1. Comparison between the results of AGM and numerical method for *g* (Left) and *f* (Right) at various *Re* and N_1 when $N_2 = N_3 = Pe_h = Pe_m = 1$.

		N_1=*Re*=1			N_1=*Re*=0.5	
η	**NUM**	**AGM**	**Error**	**NUM**	**AGM**	**Error**
-1	0.000000	0.000000	0.000000	-0.113e-3	-0.112e-3	-1.00e-06
-0.8	0.039387	0.038443	0.000944	0.017765	0.017810	-4.50e-05
-0.6	0.055363	0.052544	0.002819	0.063331	0.063317	1.40e-05
-0.4	0.060045	0.054882	0.005163	0.124830	0.124516	3.14e-04
-0.2	0.064873	0.057259	0.007614	0.190446	0.190373	7.30e-05
0.0	0.081810	0.071950	0.009860	0.248294	0.248324	-3.00e-05
0.2	0.124656	0.113092	0.011564	0.286419	0.286380	3.90e-05
0.4	0.210663	0.198378	0.012285	0.292790	0.292525	2.65e-04
0.6	0.362623	0.351256	0.011367	0.255296	0.255723	-4.27e-04
0.8	0.611554	0.603761	0.007793	0.161747	0.161912	-1.65e-04
1	1.000000	1.000000	0.000000	-0.137e-5	-0.134e-5	-3.00e-08

Table 2. Comparison between the results of VIM and numerical method for θ (Left) and ϕ (Right) at various Pe_m and Pe_h when $N_1 = N_2 = N_3 = \mathrm{Re} = 1$.

		$Pe_m = Pe_h = 1$			$Pe_m = Pe_h = 2$	
η	**NUM**	**VIM**	**Error**	**NUM**	**VIM**	**Error**
-1	1.000000	1.000000	0.000000	1.000000	1.000000	0.000000
-0.8	0.934459	0.936369	-0.001910	0.968954	0.962738	0.006216
-0.6	0.863599	0.866875	-0.003276	0.927782	0.923751	0.004031
-0.4	0.784287	0.787958	-0.003671	0.870261	0.875916	-0.005655
-0.2	0.695150	0.698154	-0.003004	0.793383	0.796308	-0.002925
0.0	0.596019	0.597650	-0.001631	0.696386	0.695300	0.001086
0.2	0.487637	0.487834	-0.000197	0.580317	0.575669	0.004648
0.4	0.371566	0.370844	0.000722	0.447988	0.441688	0.006300
0.6	0.250031	0.249117	0.000914	0.303810	0.298234	0.005576
0.8	0.125499	0.124939	0.000560	0.152995	0.149879	0.003116
1	0.000000	0.000000	0.000000	0.000000	0.000000	0.000000

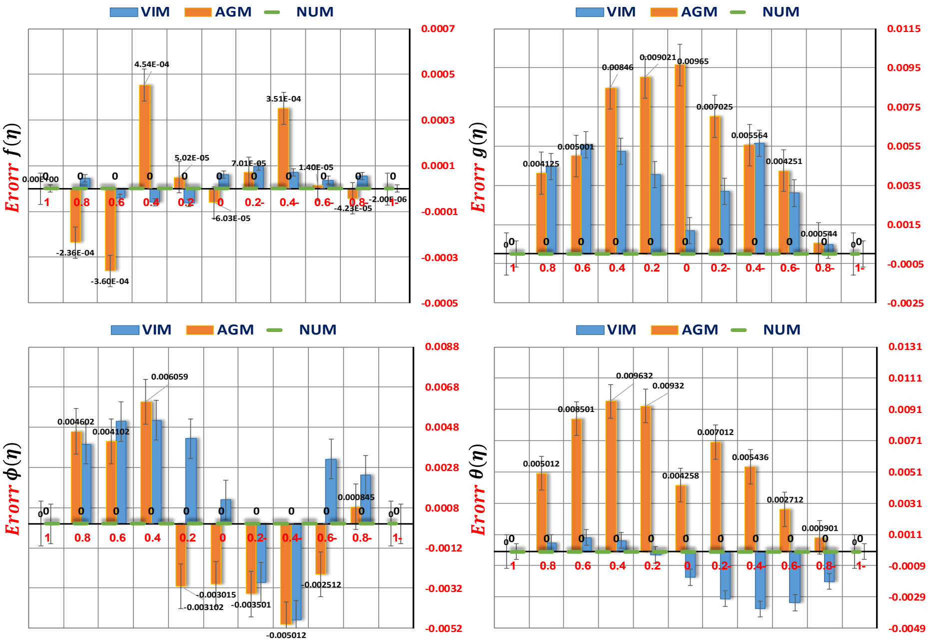

Figure 10. Comparison between the errors of VIM, AGM, and numerical (NUM) method for f (η), g (η), ∅ (η), and θ (η) when Re=1.5, $N_{1,2,3}$=0.5, Pe_m = Pe_h =0.7.

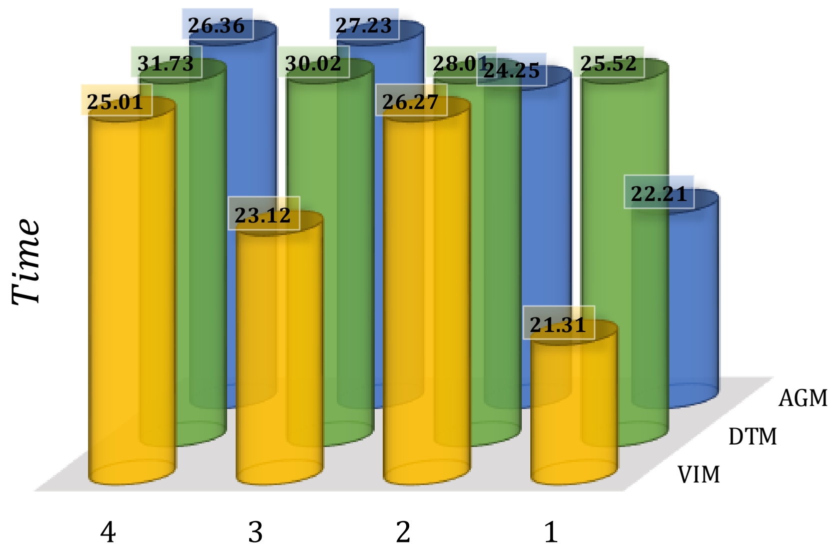

1→ $Pe_m=Pe_h=0.5,\ N_1=N_2=N_3=0.5,\ Re=0.5$

2→ $Pe_m=Pe_h=1.0,\ N_1=N_2=N_3=1.0,\ Re=0.7$

3→ $Pe_m=Pe_h=1.5,\ N_1=N_2=N_3=1.0,\ Re=1.0$

4→ $Pe_m=Pe_h=2.0,\ N_1=N_2=N_3=2.0,\ Re=1.5$

Figure 11. Comparison between the timing of VIM, AGM, and Differential Transform Method (DTM) [60] solutions at various values of active parameters.

In this paper, an analytical study on micropolar fluid flow in a two-dimensional channel with porous walls has been done using Variational Iteration Method (VIM), Akbari-Ganji's Method (AGM), and Collocation Method (CM) to acquire an exact solution of mass and heat transfer equation of steady laminar flow. In order to verify the accuracy of the present study, we have compared the results of VIM with AGM, CM, and numerical methods as well as Flex-PDE software. Figs. (2a-c) demonstrate the comparison between the outcome of VIM, CM, AGM, and Flex-PDE software. Based on these figures, the differences between the profiles are very small that means there is good compatibility between the Flex-PDE, VIM, CM, and AGM solutions. Fig. 2a indicates the variation of stream function f with η. From the lower wall to upper one, stream function increases to its maximum value and afterward it decreases. Figs. (2b) and (2c) show the variation of temperature θ and microrotation velocity g with η. As it is clear from the figures, although temperature is decreased from lower wall to the upper one, microrotation velocity is increased. Fig. 3a shows the effect of N_1 on the stream function. According to this figure, by increasing N_1, stream function increases as well. The influences of the Reynolds number (*Re*) on stream function is illustrated in Fig. 3b. It is observed that stream function decreases due to an increasing in Reynolds number. Fig. 4 demonstrates the impact of Reynolds number on microrotation velocity. In this figure, velocity boundary layer thickness decreases as Reynolds number increases. This is because of the fact that the Reynolds number shows the relative importance of inertia effect compared to the viscous effect. Figs. 5 (a-c) show the impact of N_1, N_2, and N_3 on microrotation velocity profiles. It is obvious that microrotation velocity profiles decrease by increasing N_1 and N_3, while they increase by increasing N_2. However, when

N_1>1 and N_2<1, the behavior of angular velocity is irregular and oscillatory. The impact of Peclet number (*Pe*) on concentration (ϕ) and temperature (θ) profiles is indicated in Figs. (6a) and (6b), respectively. It can be seen that by increasing Peclet number, concentration and temperature profiles increase, too. In addition, it is worth noting that with increasing Peclet number, fluctuations of temperature and concentration profiles will increase. Fig. 7a illustrates the influence of Reynolds number and Peclet number on Nusselt number (*Nu*). Results show that Nusselt number has a direct relation with Reynolds number, while it has a reverse relation with Peclet number. Fig. 7b indicates the impact of Reynolds number and Peclet number on Sherwood number (*Sh*). According to this figure, by increasing Reynolds number, Sherwood number increases, but it decreases by increasing Peclet number. Furthermore, contours of stream function, microrotation velocity, temperature, and concentration are demonstrated in Figs. (8-9). Comparison between the errors of VIM, AGM, and numerical (NUM) method for $f(\eta), g(\eta), \theta(\eta)$, and $\phi(\eta)$ at various values of active parameters is shown in Tables (1), (2), and Fig. (10). It can be seen that the error rate is very small at various values of η which are in the range of [-1, 1]. Moreover, comparison between the timing of VIM, AGM, and Differential Transform Method (DTM) [60] solutions at various values of active parameters is illustrated in Fig. (11). Regarding minor errors of VIM and AGM and their appropriate timing, as shown in Tables (1), (2), and Fig. (11), it can be said that both VIM and AGM have high accuracy in solving nonlinear differential equations.

5. CONCLUSION

In the present paper, we have used Variational Iteration Method (VIM) to study micropolar fluid flow and heat transfer in a two-dimensional permeable channel. To check the precision of the obtained results of VIM, they have been compared with the results of the numerical method (Runge-Kutta fourth-order method), Akbari-Ganji's Method (AGM), Collocation Method (CM), and Flex-PDE software. The influence of various parameters like microrotation/angular velocity, Peclet number and Reynolds number on the flow, concentration, and heat transfer distribution are studied. The main outcomes are presented in the following:

- Nusselt number (*Nu*) has a direct relation with Reynolds number (*Re*) and Sherwood number (*Sh*), while it has a reverse relation with Peclet number (*Pe*).
- Microrotation velocity profiles decrease by increasing N_1 and N_3, while they increase by increasing N_2.
- By increasing Peclet number, concentration and temperature profiles increase.
- VIM and AGM have high accuracy in solving nonlinear differential equations.

Appendix A.

Nomenclature		Greek symbols	
C	Species concentration (mol/m^3)	η	Similarity variable
k_1	Thermal conductivity (W/m.k)	μ	Dynamic viscosity (Pa.s)
g	Dimensionless microrotation velocity	ψ	Stream function (m^2/s)
(u,v)	Cartesian velocity components (m/s)	D^*	Molecular diffusivity (m^2/s)
$N_{1,2,3}$	Dimensionless parameters	h	Half of channel width (m)
Sh	Sherwood number	j	Microinertia density (m^2)
Pe	Peclet number	$\vec{N}$	Microrotation/angular velocity (m/s)
Re	Reynolds number	k	Coupling coefficient (Pa.s)
Nu	Nusselt number		
(x,y)	Cartesian coordinate components parallel and normal to channel axis, respectively		
VIM	Variational Iteration Method		

AGM	Akbari-Ganji's Method
CM	Collocation Method

Appendix B.

***Parts of Flex-PDE software codes*:**

$Coordinates\ \ Cartesian1\ \ Variables\ \ F\ \ \theta\ \ \phi\ \ g\ \ h\ \ \ Definitions\ \ 1\ \ \ N_1 = 1\ N_2 = 1\ \ N_3 = 4\ \ Re = 0.1\ \ Pe_h = 1\ \ Pe_m = 1\ \ \ Equations\ \ \ h\text{:}\ \ h = -dxx\ (F)$
$F\text{:}\ \ (1 + N_1) \times (dxx\ (h)) - N_1 \times g - Re \times (F \times dx\ (h) - dx\ (F) \times dxx\ (F)) = 0$
$G\text{:}\ \ N_2 \times (dxx\ (g)) + N_1 \times (dxx\ (F) - 2 \times g) - N_3 \times Re \times (F \times dx\ (g) - dx\ (F) \times g) = 0$
$Theta\text{:}\ \ dxx\ (\theta) + Pe_h \times (dx\ (F) \times \theta) - Pe_h \times (F \times dx\ (\theta)) = 0$
$Phi\text{:}\ \ dxx\ (\phi) + Pe_m \times (dx\ (F) \times \phi) - Pe_m \times (F \times dx\ (\phi)) = 0$
$Boundaries\ \ \ Region\ 1\ \ \ start\ (-1)\ \ \ Point\ value\ (F) = 0\ \ Point\ load\ (h) = 0$
$Point\ value\ (g) = 0\ \ \ Point\ value\ (\theta) = 1\ \ \ Point\ value\ (\phi) = 1\ \ Point\ value\ (\theta) = 0$
$Line\ to\ (1)\ \ Point\ value\ (F) = 0\ \ Point\ load\ (h) = -1\ \ Point\ value\ (g) = 1$
$Point\ value\ (\phi) = 0\ \ \ Plots\ \ Elevation\ (\phi) from\ (-1) to\ (1)$
$Elevation\ (\theta) from\ (-1) to\ (1)\ \ Elevation\ (g) from\ (-1) to\ (1)$
$Elevation\ (f)\ from\ (-1)\ to\ (1)\ \ Tecplot(\phi)\ \ \ Tecplot(\theta)\ \ Tecplot(g)\ \ Tecplot(f)$
$End.$

REFERENCES

[1] Eringen, A. C. (1966). Theory of micropolar fluids. *Journal of Mathematics and Mechanics*, 1-18.

[2] Eringen, A. C. (1972). Theory of thermomicrofluids. *Journal of Mathematical Analysis and Applications*, *38*(2), 480-496.

[3] Ariman, T. M. A. N. D., Turk, M. A., & Sylvester, N. D. (1973). Microcontinuum fluid mechanics—a review. *International Journal of Engineering Science*, *11*(8), 905-930.

[4] Lockwood, F. E., Benchaita, M. T., & Friberg, S. E. (1986). Study of lyotropic liquid crystals in viscometric flow and elastohydrodynamic contact. *ASLE transactions*, *30*(4), 539-548.

[5] Eringen, A. C. (2001). *Microcontinuum field theories: II. Fluent media* (Vol. 2). Springer Science & Business Media.

[6] Lukaszewicz, G. (1999). *Micropolar fluids: theory and applications*. Springer Science & Business Media.

[7] Gorla, R. S. R., Pender, R., & Eppich, J. (1983). Heat transfer in micropolar boundary layer flow over a flat plate. *International Journal of Engineering Science*, *21*(7), 791-798.

[8] Rees, D. A. S., & Bassom, A. P. (1996). The Blasius boundary-layer flow of a micropolar fluid. *International Journal of Engineering Science*, *34*(1), 113-124.

[9] Kelson, N. A., & Desseaux, A. (2001). Effect of surface conditions on flow of a micropolar fluid driven by a porous stretching sheet. *International Journal of Engineering Science*, *39*(16), 1881-1897.

[10] Bhargava, R., Kumar, L., & Takhar, H. S. (2003). Finite element solution of mixed convection micropolar flow driven by a porous stretching sheet. *International journal of engineering science*, *41*(18), 2161-2178.

[11] Nazar, R., Amin, N., Filip, D., & Pop, I. (2004). Stagnation point flow of a micropolar fluid towards a stretching sheet. *International Journal of Non-Linear Mechanics*, *39*(7), 1227-1235.

[12] Joneidi, A. A., Ganji, D. D., & Babaelahi, M. (2009). Micropolar flow in a porous channel with high mass transfer. *International Communications in Heat and Mass Transfer*, *36*(10), 1082-1088.

[13] Raptis, A. (1998). Flow of a micropolar fluid past a continuously moving plate by the presence of radiation. *International Journal of Heat and Mass Transfer*, *18*(41), 2865-2866.

[14] Perdikis, C., & Raptis, A. (1996). Heat transfer of a micropolar fluid by the presence of radiation. *Heat and Mass transfer, 31*(6), 381-382.

[15] Balaram, M., & Sastri, V. U. K. (1973). Micropolar free convection flow. *International Journal of Heat and Mass Transfer, 16*(2), 437-441.

[16] Mohanty, B., Mishra, S. R., & Pattanayak, H. B. (2015). Numerical investigation on heat and mass transfer effect of micropolar fluid over a stretching sheet through porous media. *Alexandria Engineering Journal*, *54*(2), 223-232.

[17] Oahimire, J. I., & Olajuwon, B. I. (2014). Effect of Hall current and thermal radiation on heat and mass transfer of a chemically reacting MHD flow of a micropolar fluid through a porous medium. *Journal of King Saud University-Engineering Sciences*, *26*(2), 112-121.

[18] Al Sakkaf, L. Y., Al-Mdallal, Q. M., & Al Khawaja, U. (2018). A Numerical Algorithm for Solving Higher-Order Nonlinear BVPs with an Application on Fluid Flow over a Shrinking Permeable Infinite Long Cylinder. *Complexity*, *2018*.

[19] Mishra, S. R., Khan, I., Al-Mdallal, Q. M., & Asifa, T. (2018). Free convective micropolar fluid flow and heat transfer over a shrinking sheet with heat source. *Case studies in thermal engineering*, *11*, 113-119.

[20] Khan, Z. H., Qasim, M., Haq, R. U., & Al-Mdallal, Q. M. (2017). Closed form dual nature solutions of fluid flow and heat transfer over a stretching/shrinking sheet in a porous medium. *Chinese journal of physics, 55*(4), 1284-1293.

[21] Elnajjar, E. J., Al-Mdallal, Q. M., & Allan, F. M. (2016). Unsteady flow and heat transfer characteristics of fluid flow over a shrinking permeable infinite long cylinder. *Journal of Heat Transfer*, *138*(9), 091008.

[22] Faltas, M. S., & Saad, E. I. (2014). Slow motion of spherical droplet in a micropolar fluid flow perpendicular to a planar solid surface. *European Journal of Mechanics-B/Fluids*, *48*, 266-276.

[23] Sheikholeslami, M., Gorji-Bandpy, M., & Soleimani, S. (2013). Two phase simulation of nanofluid flow and heat transfer using heatline analysis. *International Communications in Heat and Mass Transfer*, *47*, 73-81.

[24] Sheikholeslami, M., Gorji-Bandpy, M., & Ganji, D. D. (2013). Numerical investigation of MHD effects on Al2O3–water nanofluid flow and heat transfer in a semi-annulus enclosure using LBM. *Energy*, *60*, 501-510.

[25] Sheikholeslami, M., Bandpy, M. G., Ellahi, R., Hassan, M., & Soleimani, S. (2014). Effects of MHD on Cu–water nanofluid flow and heat transfer by means of CVFEM. *Journal of Magnetism and Magnetic Materials*, *349*, 188-200.

[26] Sheikholeslami, M., Gorji-Bandpy, M., Pop, I., & Soleimani, S. (2013). Numerical study of natural convection between a circular enclosure and a sinusoidal cylinder using control volume based finite element method. *International Journal of Thermal Sciences*, *72*, 147-158.

[27] Sheikholeslami, M., Gorji-Bandpy, M., Seyyedi, S. M., Ganji, D. D., Rokni, H. B., & Soleimani, S. (2013). Application of LBM in simulation of natural convection in a nanofluid filled square cavity with curve boundaries. *Powder Technology*, *247*, 87-94.

[28] Borrelli, A., Giantesio, G., & Patria, M. C. (2015). Magnetoconvection of a micropolar fluid in a vertical channel. *International Journal of Heat and Mass Transfer*, *80*, 614-625.

[29] Borrelli, A., Giantesio, G., & Patria, M. C. (2015). An exact solution for the 3D MHD stagnation-point flow of a micropolar fluid. *Communications in Nonlinear Science and Numerical Simulation*, *20*(1), 121-135.
[30] Joneidi, A. A., Ganji, D. D., & Babaelahi, M. (2009). Micropolar flow in a porous channel with high mass transfer. *International Communications in Heat and Mass Transfer*, *36*(10), 1082-1088.
[31] He, J. H., & Wu, X. H. (2006). Exp-function method for nonlinear wave equations. *Chaos, Solitons & Fractals*, *30*(3), 700-708.
[32] Zhang, S. (2007). Exp-function method for solving Maccari's system. *Physics Letters A*, *371*(1-2), 65-71.
[33] Wazwaz, A. M. (2004). A sine-cosine method for handlingnonlinear wave equations. *Mathematical and Computer modelling*, *40*(5-6), 499-508.
[34] Wazwaz, A. M. (2005). The tanh and the sine-cosine methods for the complex modified K dV and the generalized K dV equations. *Computers & Mathematics with Applications*, *49*(7-8), 1101-1112.
[35] Domairry, G., & Fazeli, M. (2009). Homotopy analysis method to determine the fin efficiency of convective straight fins with temperature-dependent thermal conductivity. *Communications in Nonlinear Science and Numerical Simulation*, *14*(2), 489-499.
[36] Rana, P., Shukla, N., Gupta, Y., & Pop, I. (2019). Homotopy analysis method for predicting multiple solutions in the channel flow with stability analysis. *Communications in Nonlinear Science and Numerical Simulation*, *66*, 183-193.
[37] Zhao, Y. M. (2013). F-expansion method and its application for finding new exact solutions to the kudryashov-sinelshchikov equation. *Journal of Applied Mathematics*, *2013*.
[38] Zhang, J. L., Wang, M. L., Wang, Y. M., & Fang, Z. D. (2006). The improved F-expansion method and its applications. *Physics Letters A*, *350*(1-2), 103-109.
[39] Wazzan, L. (2009). A modified tanh–coth method for solving the general Burgers–Fisher and the Kuramoto–Sivashinsky equations. *Communications in Nonlinear Science and Numerical Simulation*, *14*(6), 2642-2652.
[40] Gözükızıl, Ö. F., & Akçağıl, Ş. (2013). The tanh-coth method for some nonlinear pseudoparabolic equations with exact solutions. *Advances in Difference Equations*, *2013*(1), 143.
[41] Sheikholeslami, M., & Ganji, D. D. (2014). Ferrohydrodynamic and magnetohydrodynamic effects on ferrofluid flow and convective heat transfer. *Energy*, *75*, 400-410.
[42] Sheikholeslami, M., Soleimani, S., & Ganji, D. D. (2016). Effect of electric field on hydrothermal behavior of nanofluid in a complex geometry. *Journal of Molecular Liquids*, *213*, 153-161.
[43] Gholinia, M., Ganji, D. D., Poorfallah, M., & Gholinia, S. (2016). Analytical and Numerical Method in the Free Convection Flow of Pure Water Non-Newtonian Nano fluid between Two Parallel Perpendicular Flat Plates. *Innov Ener Res*, *5*(142), 2.
[44] Akbari, N., Gholinia, M., Gholinia, S., Dabbaghian, S., & Ganji, D. D. (2018). Analytical and Numerical Study of Hydrodynamic Nano Fluid Flow in a Two-Dimensional Semi-Porous Channel with Transverse Magnetic Field. *Sigma: Journal of Engineering & Natural Sciences/Mühendislik ve Fen Bilimleri Dergisi*, *36*(3).
[45] Akbari, N., GHOLINIA, M., Gholinia, S., Dabbaghian, S., Javadi, H., & Ganji, D. D. (2018). Analytical and Numerical Study of Micropolar Fluid Flow in a Porous Plate Due to Linear Stretching. *Sigma: Journal of Engineering & Natural Sciences/Mühendislik ve Fen Bilimleri Dergisi*, *36*(4).

[46] Ganji, S. S., Ganji, D. D., Babazadeh, H., & Sadoughi, N. (2010). Application of amplitude–frequency formulation to nonlinear oscillation system of the motion of a rigid rod rocking back. *Mathematical Methods in the Applied Sciences*, *33*(2), 157-166.

[47] Inokuti, M., Sekine, H., & Mura, T. (1978). General use of the Lagrange multiplier in nonlinear mathematical physics. *Variational method in the mechanics of solids*, *33*(5), 156-162.

[48] He, J. H. (1999). Variational iteration method–a kind of non-linear analytical technique: some examples. *International journal of non-linear mechanics*, *34*(4), 699-708.

[49] Abassy, T. A., El-Tawil, M. A., & El Zoheiry, H. (2007). Solving nonlinear partial differential equations using the modified variational iteration Padé technique. *Journal of Computational and Applied Mathematics*, *207*(1), 73-91.

[50] Abassy, T. A., El-Tawil, M. A., & El-Zoheiry, H. (2007). Exact solutions of some nonlinear partial differential equations using the variational iteration method linked with Laplace transforms and the Padé technique. *Computers & Mathematics with Applications*, *54*(7-8), 940-954.

[51] Soltani, L. A., & Shirzadi, A. (2010). A new modification of the variational iteration method. *Computers & Mathematics with Applications*, *59*(8), 2528-2535.

[52] Ren, Z. F., & He, J. H. (2009). A simple approach to nonlinear oscillators. *Physics Letters A*, *373*(41), 3749-3752.

[53] He, J. H. (2004). The homotopy perturbation method for nonlinear oscillators with discontinuities. *Applied mathematics and computation*, *151*(1), 287-292.

[54] He, J. H. (2008). An improved amplitude-frequency formulation for nonlinear oscillators. *International Journal of Nonlinear Sciences and Numerical Simulation*, *9*(2), 211-212.

[55] Sibanda, P., & Awad, F. (2010). Flow of a micropolar fluid in channel with heat and mass transfer. *Fluid Mechanics and Heat & Mass Transfer*.

[56] Sheikholeslami, M., Hatami, M., & Ganji, D. D. (2014). Micropolar fluid flow and heat transfer in a permeable channel using analytical method. *Journal of Molecular Liquids*, *194*, 30-36.

[57] Ganji, D. D., Tari, H., & Jooybari, M. B. (2007). Variational iteration method and homotopy perturbation method for nonlinear evolution equations. *Computers & Mathematics with Applications*, *54*(7-8), 1018-1027.

[58] Ganji, D. D., Afrouzi, G. A., & Talarposhti, R. A. (2007). Application of variational iteration method and homotopy–perturbation method for nonlinear heat diffusion and heat transfer equations. *Physics Letters A*, *368*(6), 450-457.

[59] Varedi, S. M., Hosseini, M. J., Rahimi, M., & Ganji, D. D. (2007). He's variational iteration method for solving a semi-linear inverse parabolic equation. *Physics letters A*, *370*(3-4), 275-280.

[60] Sheikholeslami, M., Ashorynejad, H. R., Ganji, D. D., & Rashidi, M. M. (2014). Heat and mass transfer of a micropolar fluid in a porous channel. *Communications in Numerical Analysis*, *2014*(unknown), 1-20.